CORRESPONDENCE:

Multi-century evaluation of Sierra Nevada snowpack

To the Editor — California is currently experiencing a record-setting drought that started in 2012 and recently culminated in the first ever mandatory state-wide water restriction[1]. The snowpack conditions in the Sierra Nevada mountains present an ominous sign of the severity of this drought: the 1 April 2015 snow water equivalent (SWE) was at only 5% of its historical average[2]. In the Mediterranean climate of California, with 80% of the precipitation occurring during winter months, Sierra Nevada snowpack plays a critical role in replenishing the state's water reservoirs and provides 30% of its water supply[3]. As a result, a multi-year and severe snowpack decline can acutely impact human and natural systems, including urban and agricultural water supplies, hydroelectric power[4] and wildfire risk[5].

The exceptional character of the 2012–2015 drought has been revealed in millennium-length palaeoclimate records[6], but no long-term historical context is available for the recent snowpack decline. Here, we present an annually resolved reconstruction of 1 April SWE conditions over the whole Sierra Nevada range for the past 500 years (Fig. 1). We combined an extensive compilation of blue oak tree-ring series that reflects large-scale California winter precipitation anomalies[7] (Supplementary Information and Supplementary Fig. 1) with a tree-ring-based California February–March temperature record[8] in a reconstruction that explains 63% of the Sierra Nevada SWE variance over the instrumental period (Supplementary Table 1). Our reconstruction shows strong statistical skill (Supplementary Table 2), but underestimates anomalously high SWE values over the instrumental period (for example, in 1952 and 1969). However, SWE lows (for example, in 1934 and 1977) are reliably captured and our reconstruction reveals that the 2015 low is unprecedented in the context of the past 500 years (Fig. 1). Our error estimation indicates that there is a possibility that a few (primarily sixteenth century) years exceeded the 2015 low, but the estimated return interval for the 2015 SWE value — as calculated based on a generalized extreme value (GEV) distribution (Supplementary Information) — is 3,100 years and confirms its exceptional character. GEV-estimated return intervals

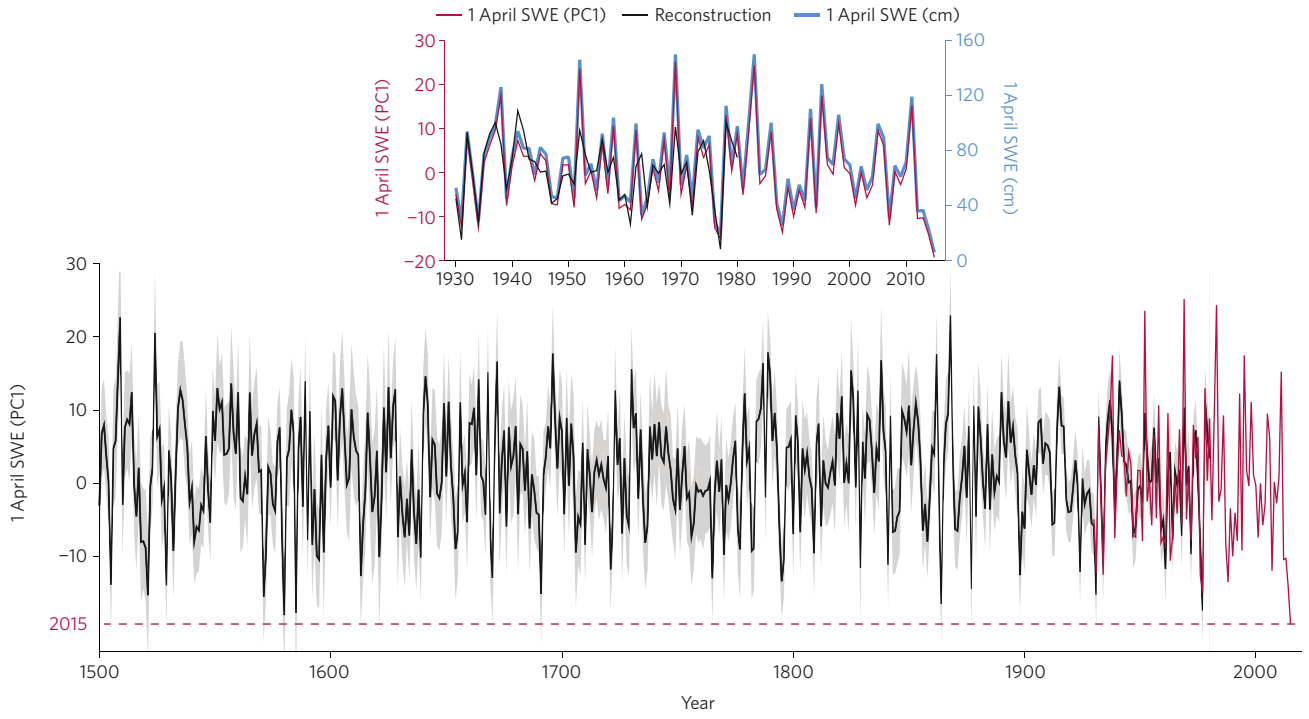

Figure 1 | Sierra Nevada 1 April snow water equivalent reconstruction (1500–1980). Bottom: instrumental (1930–2015; red curve) and reconstructed (1500–1980; black curve) first Principal Component (PC1) of Sierra Nevada 1 April snow water equivalent (SWE) values. The SWE reconstruction was calibrated against the PC1 of 1 April SWE measurements from 108 Sierra Nevada stations and explains 63% of its variance over the period of overlap (1930–1980; top). The 108-station average SWE value (in cm; 1930–2015) is plotted for comparison (blue curve; top). The grey shading around the reconstruction (bottom) indicates the combined error estimation (Supplementary Information). The 2015 SWE value is indicated by the red dashed line.

can have large confidence intervals (Supplementary Fig. 2), but the 2015 SWE value exceeds the 95% confidence interval for a 500-year return period (Supplementary Fig. 3). In comparison, the previous lowest SWE reading (in 1977) exceeds the 95% confidence interval for only a 60-year return period. We also find that the 2015 SWE value is strongly exceptional — exceeding the 95% confidence interval for a 1,000-year return period — at low-elevation Sierra Nevada sites where winter temperature has strong control over SWE[9], but less so at high-elevation sites, where it exceeds the 95% confidence interval for only a 95-year return period (Supplementary Information and Supplementary Fig. 2).

The 2015 record low snowpack coincides with record high California January–March temperatures[10] and highlights the modulating role of temperature extremes in Californian drought severity. Snowpack lows, among other drought metrics, are driven by the co-occurrence of precipitation deficits and high temperature extremes[11], and we find that the exacerbating effect of warm winter temperatures[12] is stronger at low than at high Sierra Nevada elevations. Anthropogenic warming is projected to further increase the probability of severe drought events[13], advance the timing of spring snowmelt and increase rain-to-snow ratios[14]. The ongoing and projected role of temperature in the amount and duration of California's primary natural water storage system thus foreshadows major future impacts on the state's water supplies. ❐

References

1. Brown, E. G. J. *Executive Order B-29-15* (Executive Department State of California, 2015).
2. Natural Resources Conservation Service *Snow Course Measurements for April 2015* (California Department of Water Resources, 2015); http://cdec.water.ca.gov/cgi-progs/snow/COURSES.04
3. *040115 Snow Survey* (California Department of Water Resources, 2015).
4. Bartos, M. D. & Chester, M. V. *Nature Clim. Change* **5,** 748–752 (2015).
5. Westerling, A. L., Hidalgo, H. G., Cayan, D. R. & Swetnam, T. W. *Science* **313,** 940–943 (2006).
6. Griffin, D. & Anchukaitis, K. J. *Geophys. Res. Lett.* **41,** 2014GL062433 (2014).
7. Stahle, D. W. *et al. Earth Interact.* **17,** 1–23 (2013).
8. Wahl, E. R., Diaz, H. F., Smerdon, J. E. & Ammann, C. M. *Glob. Planet. Change* **122,** 238–250 (2014).
9. Howat, I. M. & Tulaczyk, S. *J. Geophys. Res. Earth* **110,** 151–156 (2005).
10. National Climatic Data Center *State of the Climate: National Overview for March 2015* (NOAA, 2015); http://www.ncdc.noaa.gov/sotc/summary-info/national/201503
11. Diffenbaugh, N. S., Swain, D. L. & Touma, D. *Proc. Natl Acad. Sci. USA* **112,** 3931–3936 (2015).
12. Mao, Y., Nijssen, B. & Lettenmaier, D. P. *Geophys. Res. Lett.* **42,** 2805–2813 (2015).
13. Cook, B. I., Ault, T. R. & Smerdon, J. E. *Science Advances* **1,** e1400082 (2015).
14. Ashfaq, M. *et al. J. Geophys. Res. Atmos.* **118,** 10676–10693 (2013).

Acknowledgements

This work was supported by a National Science Foundation CAREER grant (AGS-1349942), a grant from the Department of the Interior Southwest Climate Science Center (US Geological Survey; G13AC00339) and a Swiss National Science Foundation grant (P300P2_154543). We are grateful to Kevin Anchukaitis for discussion and useful input.

Additional information

Supplementary information is available in the online version of the paper.

Author contributions

S.B., F.B. and V.T. conceived and designed the study, and wrote the Correspondence with input from E.R.W. and D.W.S. E.R.W. and D.W.S. contributed data and S.B. and F.B. performed the analyses with input from V.T. All authors contributed to the interpretation of the data set and discussion.

Soumaya Belmecheri[1], Flurin Babst[1], Eugene R. Wahl[2], David W. Stahle[3] and Valerie Trouet[1]*

[1]Laboratory of Tree-Ring Research, University of Arizona, Tucson, Arizona 85721, USA, [2]NOAA/National Centers for Environmental Information, Paleoclimatology Group, Boulder, Colorado 80305, USA, [3]Department of Geosciences, University of Arkansas, Fayetteville, Arkansas 72701, USA.
*e-mail: trouet@ltrr.arizona.edu

Published online: 14 September 2015

nature climate change

SUPPLEMENTARY INFORMATION

DOI: 10.1038/NCLIMATE2809

CORRESPONDENCE:

Multi-century evaluation of Sierra Nevada snowpack

Authors: Soumaya Belmecheri[1], Flurin Babst[1], Eugene R. Wahl[2], David W. Stahle[3], and Valerie Trouet[1*]

[1]Laboratory of Tree-Ring Research, University of Arizona, Tucson, Arizona, USA.

[2]NOAA/National Centers for Environmental Information, Paleoclimatology Group, Boulder, Colorado, USA.

[3]Department of Geosciences, University of Arkansas, Fayetteville, Arkansas, USA.

* To whom correspondence should be addressed (email: trouet@ltrr.arizona.edu)

Content of this file:

Material and Methods

Snowpack data

A dataset of April 1 snow water equivalent (subsequently abbreviated as SWE) was compiled from two existing datasets for the Sierra Nevada (SN), California (CA): the National Resources Conservation Service (NRCS) and Water Climate Center (www.wcc.nrcs.usda.gov/snow/) and the California Department of Water Resources (http://cdec.water.ca.gov/misc/SnowCourses.html). A total of 108 SN stations that span at least the period 1930-2015 CE (Table S1) and with less than 10 % missing data were used. These stations contained 2.5 % missing values, spread across stations and years. For a given year, missing values were replaced with the average SWE value of all other

DOI: 10.1038/NCLIMATE2809

The gapfilled SWE station time series (1930-2015 CE) were positively and significantly inter-correlated over the period of record (mean inter-series correlation (RBAR) = 0.8, $p<0.0001$). To extract common variability of the 108 individual station time series, we performed a principal component analysis using the FacftorMine R package for multivariate analyses[1]. The resulting first principal component ($PC1_{SWE}$) explained 78% of the common variance and was selected as the instrumental target for our SWE reconstruction. All individual stations had a loading >0.7 on this first PCA axis.

Proxy data

We included two proxy time series as SWE predictors in our reconstruction model. The first proxy consisted of a compilation of 1,935 publicly available individual blue oak (*Quercus douglasii*) tree-ring width series from 1505 trees at 33 sites[2] in central CA that were combined[3] into one master chronology. This chronology had a mean segment length (MSL) of 161 years and a RBAR of r = 0.64 (Fig. S1). The geometric age-trend was removed from all raw series using cubic smoothing spline detrending with a 50% frequency-response cutoff at two thirds of MSL (106 year [4]). A master chronology was then calculated by averaging the detrended series using a biweight robust mean[5]. We corrected this regional chronology for variance changes due to changes in sample replication over time[6]. The final chronology spanned the period 1379-2005 CE and had an estimated population signal (EPS[7]) above the commonly utilized, but arbitrary, threshold of 0.85 from 1405 onwards. It is worth noting that the Griffin and Anchukaitis[8] CA precipitation reconstruction is also based on blue oak tree-ring data, but their data set was limited to 273 trees from four sites and the overlap with our data set is limited to less than 13% of the trees and 9% of the sites.

The second proxy was derived from a February-March (FM) temperature field reconstruction[9] (1500-1980 CE) as the mean of two 5 x 5 degree grid cells located over central and southern CA. These two cells are those of the four grid cells that are primarily located in California from the gridded FM temperature field reconstruction[9] that had complete data coverage throughout the full independent validation period (1875-1903 CE)[10]. The two grid cell temperature reconstructions are well validated (RE = 0.27 and 0.33, respectively, for central and southern CA). The FM temperature reconstruction represents the only combination of successful calibration and validation performance for spatially-explicit reconstruction of the western North America temperature field from a suite of sub-annual periods evaluated, including DJF, JFM, and varieties of growing season. It has been shown to closely track DJF spatial ENSO characteristics in western North America, for both El Niño and La Niña conditions[9], providing an independent confirmation of its fidelity to represent winter conditions in the CA region. More generally, the FM period, per se, closely tracks the trajectory of temperature conditions during the overall snow delivery season to the SN, November-March (NDJFM), immediately preceding the official 1 April SWE measurement date. Based on instrumental data for 1896-2015 CE from NOAA's National Centers for Environmental Information (NCEI, http://www.ncdc.noaa.gov/cag/, accessed 10 and 13 July, 2015), Pearson's r between the FM and NDJFM temperature averages for CA is 0.82; between FM and DJFM $r = 0.84$, and between FM and JFM $r = 0.9$ ($p<0.001$ for all).

It is important to note that the two predictor time series are fully independent of each other. There is no overlap of the tree-ring chronologies employed in the FM temperature reconstruction and the blue oak master chronology. The two data sets are also statistically independent of each other (r=0.0003).

DOI: 10.1038/NCLIMATE2809

April 1 SWE reconstruction

The calibration period for our SWE reconstruction (1930-1980 CE) was defined by the period of overlap of the instrumental and proxy data. We used a stepwise multiple linear regression model with the two proxy time series as predictors for the $PC1_{SWE}$ target. This model explained 63 % (58% by the blue oak time series, $p < 0.001$; 5% by the temperature reconstruction, $p < 0.05$) of the variance in $PC1_{SWE}$ and we verified its reconstruction skill based on two rounds of cross-calibration-verification tests. In a first round, we split the calibration period into two equal portions (1930-1955 CE; 1956-1980 CE), developed a stepwise multiple linear regression model for each of the sub-periods, and derived reduction of error (RE) and coefficient of efficiency (CE) statistics[11] for both periods (Table S2, all stations). In a second round, we calculated RE and CE based on leave-one-out subsets of the calibration period. The resulting values ranged from 0.61 to 0.66 with a mean of 0.64, thus indicating that our calibration model has strong reconstruction skill.

Uncertainty estimation of the April 1 SWE reconstruction

Uncertainty in the SWE reconstruction arises from (1) the detrending of the blue oak tree-ring series (detrending error), (2) the decreasing number of tree-ring series back through time in the tree-ring proxy (replication error), (3) uncertainty in the FM temperature field reconstruction, and (4) unexplained variance in the stepwise multiple linear regression model (calibration error[12]).

The detrending error is a representation of the centennial-scale climatic signal uncertainty in the blue oak trees and was calculated using a subset chronology that was based on a subset (n=104) of the blue oak tree-ring data set (RBAR=0.658; MSL=336; EPS > 0.85 for 1500-1980 CE; Fig. S1). We detrended each series of this subset with a 336-yr cubic smoothing spline – equaling the full

MSL- and developed a subset chronology according to the procedure described above in the *Proxy Data* section. We developed this subset chronology in an attempt to preserve a maximum amount of low-frequency signal and the difference between the full (MSL=106) and subset (MSL=336) chronology values for each year was utilized to represent the detrending error.

We estimated the replication error by bootstrapping[13]: standardized tree-ring measurements for every year were sampled with replacement 1000 times and arithmetic means were calculated. Two-tailed 95% confidence intervals (CI) were estimated based on the distribution of the bootstrapped mean and the upper and lower limits of the CI were used as the replication error boundaries. Uncertainty in the FM temperature reconstruction was estimated as the 95% probability ranges of the reconstruction uncertainty ensemble[9,10]. The calibration error was estimated as the standard error (SE) for the full calibration period 1930–1980 CE.

Finally, the overall error for the SWE reconstruction was estimated as the square root of the standardized summed and squared detrending, replication, temperature reconstruction, and calibration error terms and scaled to the amplitude of the $PC1_{SWE}$ target.

Estimation of the return interval of the 2015 SWE level

To contextualize the record low 2015 SWE value, we used the R package extRemes to estimate its return interval based on a generalized extreme value (GEV[14]) distribution over the preceding five centuries (i.e., 1500-2014 CE). For this purpose, we merged the SWE reconstruction with the $PC1_{SWE}$ instrumental target, using the instrumental data for the period of overlap (1930-1980 CE). A univariate GEV distribution was fitted to the data using a maximum likelihood approach[15] to identify extreme $PC1_{SWE}$ values, their expected return intervals (represented by the quantiles of the GEV), and 95% confidence intervals around the estimated return intervals (Figure S2).

DOI: 10.1038/NCLIMATE2809

April 1 SWE reconstruction and estimation of the return interval for low and high elevation sites.

To assess altitudinal differences in the return interval of the 2015 SWE value, we calculated the GEV[14] separately for SWE reconstructions for low and high elevation stations (Fig S3) following the same methodology described above for the primary SWE reconstruction. For this purpose, we selected stations with altitudes in the lower quartile (altitude < 2129.8 m) and the upper quartile (altitude > 2669.2 m) and calculated two new PC-based reconstruction targets containing 27 stations each ($PC1_{Low}$ and $PC1_{High}$; Table S1). The resulting first principal components explained 82% and 86% of the common variance, respectively. Our two predictor proxy time series explained 67% (64% ($p < 0.001$) and 3% ($p < 0.1$) by the blue oak time series and the temperature reconstruction respectively) of the variance in $PC1_{High}$ and 50% (40% ($p < 0.001$) and 10% ($p < 0.01$) respectively) of the variance in $PC1_{Low}$ over the 1930-1980 CE calibration period. Both the high and low elevation models show strong reconstruction skills (Table S2).

Supplementary Tables

Table S1 Site description for 108 Sierra Nevada (California) April 1 SWE stations used for the instrumental target ($PC1_{SWE}$). Stations highlighted in bold indicate stations in the lower and upper elevation quartiles used for $PC1_{Low}$ and $PC1_{High}$.

Site	Latitude N	Longitude E	Elevation m.a.s.l	Period of record CE	Average April 1 SWE (cm)
CHF	**40.283**	**-121.25**	**1402.08**	**1930-2015**	**15.2**
WRN	**40.387**	**-121.31**	**1554.48**	**1930-2015**	**37.3**
SPD	**39.317**	**-120.642**	**1584.96**	**1927-2015**	**54.1**
FEM	**40.355**	**-121.422**	**1645.92**	**1930-2015**	**58.7**
MSV	**40.293**	**-121.292**	**1706.88**	**1931-2015**	**37.3**
BOM	**39.458**	**-120.6**	**1722.12**	**1927-2015**	**56.6**
CCO	**39.303**	**-120.543**	**1798.32**	**1918-2015**	**70.1**
MLF	**39.942**	**-121.19**	**1798.32**	**1930-2015**	**99.1**
20H08	**41.23**	**-120.79**	**1886.712**	**1930-2015**	**31.2**
ADI	**41.237**	**-120.793**	**1889.76**	**1930-2015**	**31.8**
HRF	**40.418**	**-121.275**	**1889.76**	**1930-2015**	**72.4**
3LK	**39.973**	**-121.213**	**1905**	**1930-2015**	**103.6**
19L01	**38.88**	**-119.98**	**1949.501**	**1930-2015**	**17.4**
GFR	**36.57**	**-118.768**	**1950.72**	**1930-2015**	**37.3**
UTR	**38.873**	**-119.983**	**1950.72**	**1930-2015**	**17.8**
FOD	**39.36**	**-120.5**	**1981.2**	**1918-2015**	**103.9**
FNP	**39.47**	**-120.572**	**1981.2**	**1927-2015**	**75.7**
BHV	**37.995**	**-119.78**	**1981.2**	**1930-2015**	**59.7**
NGF	**38.327**	**-119.912**	**1981.2**	**1930-2015**	**49.8**
20K07	**39.35**	**-120.5**	**1981.2**	**1918-2015**	**95.1**
20K08	**39.35**	**-120.5**	**2011.68**	**1918-2015**	**114.5**
FNF	**39.355**	**-120.503**	**2042.16**	**1918-2015**	**122.9**
BV1	**38.618**	**-120.228**	**2042.16**	**1930-2015**	**62.5**
CHU	**39.682**	**-120.623**	**2042.16**	**1931-2015**	**78.0**
DNS	**39.31**	**-120.338**	**2103.12**	**1910-2015**	**98.0**
20K10	**39.32**	**-120.33**	**2103.12**	**1910-2015**	**93.8**
FDM	**37.023**	**-119.08**	**2118.36**	**1930-2015**	**54.1**
WR2	39.142	-120.225	2133.6	1913-2015	106.2
WBB	39.485	-120.425	2133.6	1925-2015	80.5
GFL	37.765	-119.773	2133.6	1930-2015	81.3
HTT	37.228	-119.222	2133.6	1930-2015	47.2
PGM	37.667	-119.625	2133.6	1931-2015	74.4
20K02	39.48	-120.43	2133.6	1925-2015	79.5
20H06	41.58	-120.3	2148.84	1930-2015	40.7
ENM	39.436	-120.525	2164.08	1927-2015	115.3
CDP	41.583	-120.303	2164.08	1930-2015	42.4

DOI: 10.1038/NCLIMATE2809

Site	Latitude N	Longitude E	Elevation m.a.s.l	Period of record CE	Average April 1 SWE (cm)
SIL	38.678	-120.118	2164.08	1930-2015	53.3
19L02	38.87	-119.96	2173.834	1930-2015	26.4
CHM	37.41	-119.49	2179.32	1930-2015	93.0
RDM	39.343	-120.508	2194.56	1918-2015	131.8
MWL	39.417	-120.508	2194.56	1920-2015	141.7
FLC	37.277	-118.962	2194.56	1930-2015	17.8
RLD	38.28	-119.73	2209.8	1930-2015	50.5
FBN	38.85	-119.95	2225.04	1930-2015	26.4
CKT	37.408	-119.48	2270.76	1930-2015	93.5
RP2	39.001	-120.14	2286	1912-2015	78.2
PFV	38.517	-119.9	2286	1930-2015	98.8
EGM	38.288	-119.832	2286	1931-2015	61.5
BMS	36.715	-118.842	2316.48	1930-2015	62.5
HCM	36.752	-118.75	2316.48	1930-2015	41.4
BHM	36.122	-118.293	2331.72	1930-2015	21.1
WPK	39.483	-120.44	2377.44	1923-2015	106.4
MSH	41.372	-122.23	2407.92	1930-2015	136.1
BLK	38.613	-119.931	2438.4	1918-2015	91.9
20K01	39.48	-120.43	2438.4	1922-2015	106.8
REL	38.243	-119.758	2468.88	1931-2015	100.6
TNY	37.838	-119.448	2484.12	1930-2015	85.3
20L04	38.86	-120.11	2495.702	1913-2015	147.7
LLL	38.86	-120.112	2499.36	1913-2015	150.1
PRM	37.122	-118.895	2499.36	1930-2015	66.8
19L09	38.26	-119.46	2508.809	1925-2015	25.2
WLF	38.275	-119.45	2514.6	1925-2015	22.9
HLM	37.122	-119.005	2514.6	1930-2015	67.8
LLP	40.467	-121.508	2514.6	1930-2015	203.7
MMT	37.62	-118.992	2529.84	1931-2015	51.3
SMD	36.943	-118.913	2529.84	1930-2015	82.0
BNM	36.038	-118.328	2529.84	1930-2015	34.5
HKM	36.382	-118.655	2590.8	1930-2015	69.9
LWM	36.378	-118.347	2590.8	1930-2015	32.8
LMD	37.13	-118.92	2590.8	1930-2015	74.4
UCP	38.695	-119.983	2590.8	1930-2015	91.9
19L04	38.7	-119.99	2597.506	1930-2015	85.1
PTM	36.588	-118.717	2621.28	1925-2015	93.2
TUM	37.873	-119.35	2621.28	1930-2015	57.7
RC1	37.492	-118.717	2651.76	1926-2015	17.8
RMM	36.352	-118.265	2651.76	1930-2015	29.2
SNF	37.827	-119.497	2651.76	1930-2015	113.0

Site	Latitude N	Longitude E	Elevation m.a.s.l	Period of record CE	Average April 1 SWE (cm)
WDH	37.025	-118.908	2682.24	1930-2015	80.0
RWM	36.717	-118.737	2697.48	1933-2015	67.3
MRO	39.353	-119.898	2743.2	1910-2015	90.4
MN2	37.663	-119.017	2743.2	1929-2015	73.9
RMD	35.965	-118.36	2743.2	1930-2015	61.2
RC2	37.473	-118.717	2758.44	1926-2015	27.9
KSR	37.295	-119.102	2773.68	1930-2015	99.1
MAM	37.61	-119.033	2834.64	1931-2015	106.4
NTH	37.228	-118.62	2834.64	1930-2015	25.9
AGP	37.724	-119.143	2880.36	1930-2015	80.8
BP2	37.127	-118.47	2956.56	1926-2015	37.6
UBC	37.184	-118.938	2956.56	1929-2015	96.0
BP3	37.128	-118.475	2987.04	1926-2015	46.5
DAN	37.897	-119.257	2987.04	1927-2015	79.0
BMD	37.113	-118.837	2987.04	1930-2015	84.6
19M01	37.92	-119.25	3017.52	1926-2015	67.6
BP1	37.125	-118.483	3048	1926-2015	57.4
RC3	37.45	-118.742	3048	1926-2015	37.3
CW1	36.483	-118.177	3093.72	1926-2015	31.2
SWM	37.162	-118.563	3108.96	1927-2015	48.3
BCB	37.067	-118.77	3139.44	1930-2015	86.6
EPP	37.235	-118.687	3291.84	1930-2015	38.6
CW2	36.483	-118.217	3383.28	1926-2015	35.8
BSH	37.1	-118.557	3413.76	1930-2015	88.9
PPS	37.24	-118.687	3444.24	1930-2015	96.3

DOI: 10.1038/NCLIMATE2809

Table S2 Calibration and verification statistics for the SN April 1 SWE reconstructions.

Stations	Period	Calibration	Verification		
		R^2	R^2	RE	CE
All	1930-1980 CE	0.63			
	1930-1955 CE	0.66	0.62	0.61	0.60
	1956-1980 CE	0.63	0.65	0.63	0.62
Subset high elevation	1930-1980 CE	0.67			
	1930-1955 CE	0.69	0.68	0.62	0.61
	1956-1980 CE	0.68	0.66	0.51	0.50
Subset low elevation	1930-1980 CE	0.50			
	1930-1955 CE	0.55	0.46	0.52	0.52
	1956-1980 CE	0.47	0.54	0.42	0.41

Supplementary Figures

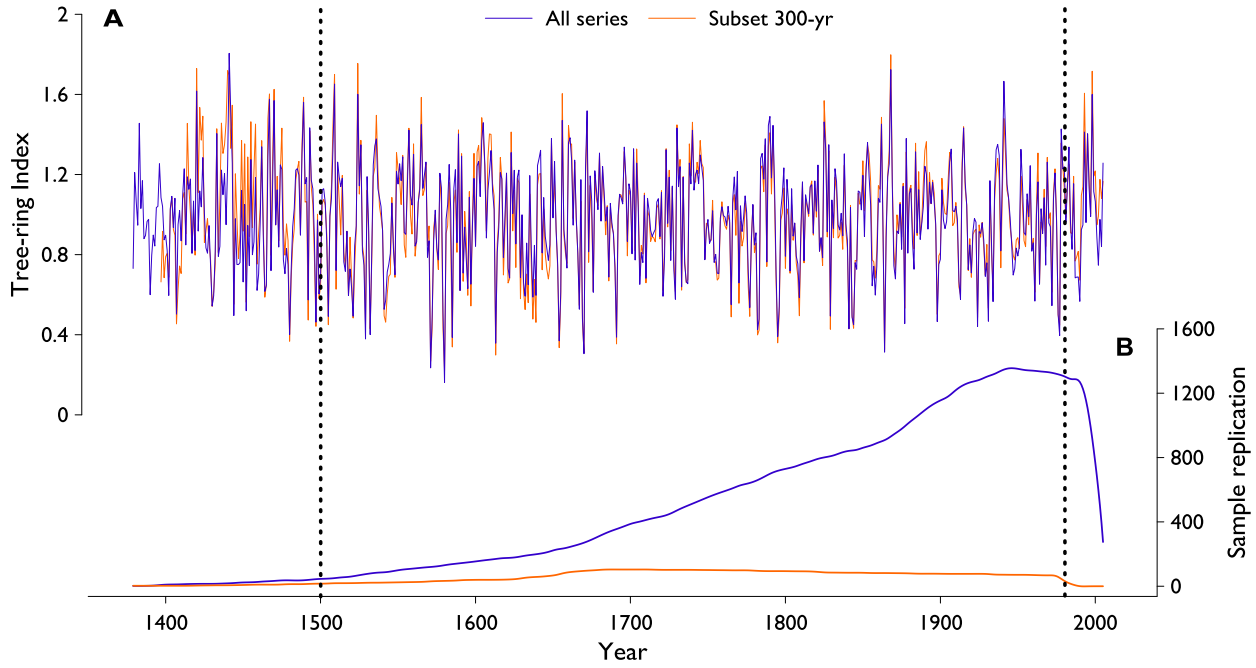

Figure S1: **Blue oak chronology used to reconstruct April 1 snow water equivalent (SWE) in the Sierra Nevada, California.** The master chronologies based on the full dataset (blue line; n = 1935 series from 1505 trees; mean segment length (MSL) = 161 years) and a subset thereof (orange line; n = 104 series; MSL = 336 years) geared at maximizing MSL for detrending error estimation are shown in panel A. Sample replication over time for both chronologies is shown in panel B. Vertical dashed lines demarcate the reconstruction period (1500-1980 CE). Sample replication of the full data set master chronology was 45 series from 31 trees in 1500 CE.

DOI: 10.1038/NCLIMATE2809

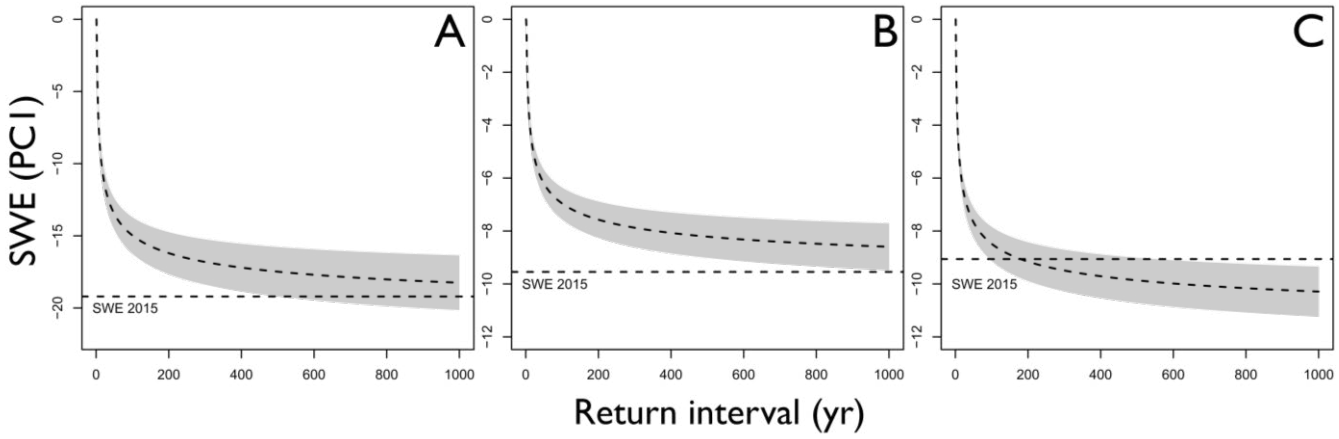

Figure S2: **GEV estimated return intervals of April 1 snow water equivalent (SWE) in the Sierra Nevada, California.** The estimates are based on a generalized extreme value (GEV) distribution of the combined instrumental and reconstructed (1500-2014 CE) first principal component (PC1) of SWE from 108 observational stations ($PC1_{SWE}$; A), from low elevation stations (< 2129.8 m) ($PC1_{Low}$; B) and high elevation stations (> 2669.2 m) ($PC1_{High}$; C) . The grey shaded area represents the 95% confidence interval around the mean return levels and the 2015 SWE is indicated by a horizontal dashed line.

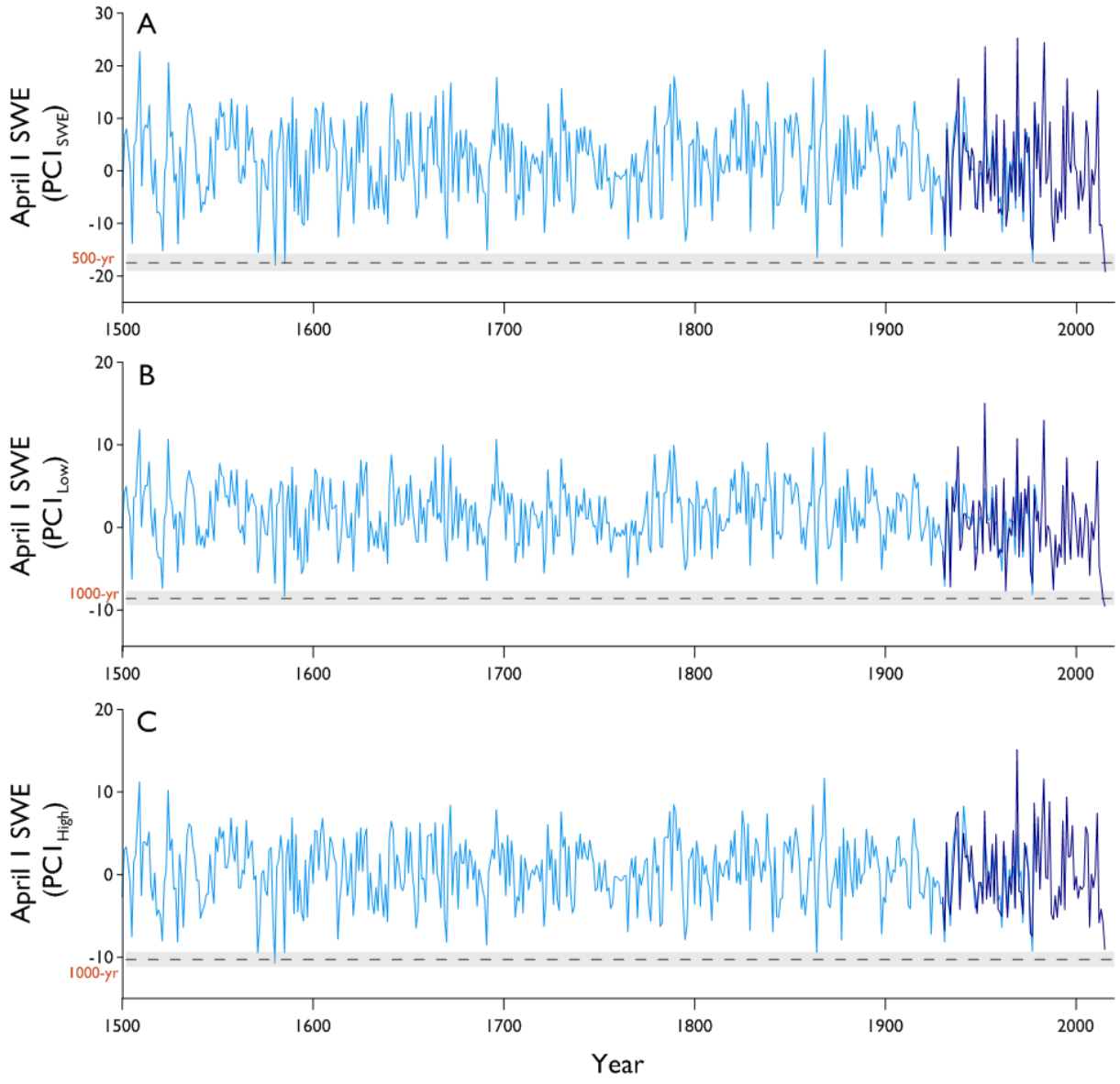

Figure S3: **Sierra Nevada April 1 snow water equivalent reconstruction (1500-1980 CE).** Instrumental (1930-2015 CE; dark blue curve) and reconstructed (1500-1980 CE; light blue curve) first Principal Components of 108-stations ($PC1_{SWE}$ [A]), of low elevation ($PC1_{Low}$, [B]) and high elevation ($PC1_{High}$, [C]) sites of Sierra Nevada (SN) April 1 snow water equivalent (SWE) values. The horizontal dashed line and surrounding grey shading indicate the SWE level and 95% confidence intervals for a 500-yr [A] and 1000-yr [B,C] return period estimated based on the generalized extreme value distribution over 1500-2014 CE.

DOI: 10.1038/NCLIMATE2809

References

1 Sébastien Lê, J. J., François Husson. FactoMineR: An R Package for Multivariate Analysis. . *Journal of Statistical Software* **25** (2008).

2 Stahle, D. W. *et al.* The Ancient Blue Oak Woodlands of California: Longevity and Hydroclimatic History. *Earth Interactions* **17**, 1-23, doi:10.1175/2013EI000518.1 (2013).

3 Trouet, V. A Tree-Ring Based Late Summer Temperature Reconstruction (AD 1675–1980) for the Northeastern Mediterranean. *Radiocarbon* **56**, 69-78, doi:http://dx.doi.org/10.2458/azu_rc.56.18323 (2014).

4 Cook, E. R. & Peters, K. The smoothing spline: A new approach to standardizing forest interior tree-ring width series for dendroclimatic studies. *Tree-Ring Bulletin* **41** (1981).

5 Cook, E. R. & Peters, K. Calculating unbiased tree-ring indices for the study of climatic and environmental change. *Holocene* **7**, 361-370 (1997).

6 Frank, D., Esper, J. & Cook, E. R. Adjustment for proxy number and coherence in a large-scale temperature reconstruction. *Geophysical Research Letters* **34**, n/a-n/a, doi:10.1029/2007GL030571 (2007).

7 Wigley, T. M. L., Briffa, K. R. & Jones, P. D. ON THE AVERAGE VALUE OF CORRELATED TIME-SERIES, WITH APPLICATIONS IN DENDROCLIMATOLOGY AND HYDROMETEOROLOGY. *Journal of Climate and Applied Meteorology* **23**, 201-213, doi:10.1175/1520-0450(1984)023<0201:otavoc>2.0.co;2 (1984).

8 Griffin, D. & Anchukaitis, K. J. How unusual is the 2012–2014 California drought? *Geophysical Research Letters* **41**, 2014GL062433, doi:10.1002/2014GL062433 (2014).

9 Wahl, E. R., Diaz, H. F., Smerdon, J. E. & Ammann, C. M. Late winter temperature response to large tropical volcanic eruptions in temperate western North America: Relationship to ENSO phases. *Global and Planetary Change* **122**, 238-250 (2014).

10 Wahl, E. R. & Smerdon, J. E. Comparative performance of paleoclimate field and index reconstructions derived from climate proxies and noise-only predictors. *Geophysical Research Letters* **39**, n/a-n/a, doi:10.1029/2012GL051086 (2012).

11 Cook, E. R., Briffa, K. R. & Jones, P. D. Spatial regression methods in dendroclimatology - a review and comparison of 2 techniques. *International Journal of Climatology* **14**, 379-402 (1994).

12 Esper, J., Frank, D., Buentgen, U., Verstege, A. & Luterbacher, J. Long-term drought severity variations in Morocco. *Geophysical Research Letters* **34**, doi:L1770210.1029/2007gl030844 (2007).

13 Briffa, K. R. *et al.* Fennoscandian summers from ad 500: temperature changes on short and long timescales. *Clim Dynam* **7**, 111-119, doi:10.1007/BF00211153 (1992).

14 de Haan, L. a. F., A. *Extreme Value Theory: An Introduction*. (Springer, 2006).

15 Martins, E. S. & Stedinger, J. R. Generalized maximum-likelihood generalized extreme-value quantile estimators for hydrologic data. *Water Resources Research* **36**, 737-744, doi:10.1029/1999WR900330 (2000).